

Semi-automated synthesis, validation and microPET imaging of ^{18}F -FP-DTBZ as a vesicular monoamine transporter ligand

CHEN Zhengping* LIU Chunyi LI Xiaomin TANG Jie TAN Cheng
HUANG Hongbo YU Huixin LUO Shineng

Key Laboratory of Nuclear Medicine, Ministry of Health, Jiangsu Key Laboratory of Molecular Nuclear Medicine,
Jiangsu Institute of Nuclear Medicine, Wuxi 214063, China

Abstract This work was to develop a semi-automated synthesis of ^{18}F -9-fluoropropyl-9-desmethyl-DTBZ (^{18}F -FP-DTBZ) and validate its potential as a vesicular monoamine transporter 2 (VMAT2) ligand. ^{18}F -FP-DTBZ was synthesized by a semi-automated procedure in a 21–35% yield without decay correction and with a radiochemical purity of >98%. Bioistribution in rats exhibited a favorable brain uptakes of the ligand (0.31 ± 0.04 ID% at 60 min post injection, $n=8$). The highest radioactivity located in VMAT2 enriched striatal tissue. The target-to-nontarget ratio (striatum/cerebellum, ST/CB) was 4.81 ± 0.84 . Blocking studies implied that striatum uptake could be blocked by DTBZ (a VMAT2 inhibitor) but could not by CFT (a dopamine transporter inhibitor). MicroPET imaging with ^{18}F -FP-DTBZ in normal rats gave high quality images in which high radioactivity were observed in the striatal tissue. Time-and-activity curves revealed good retention in the target (striatum) and rapid clearance in the background (cerebellum), which resulted in a maximum ST/CB ratio of 5.08 ± 0.81 ($n=3$) in 80–120 min. By contrast, the 6-hydroxydopamine unilateral lesioned rats gave asymmetrical striata images with higher ^{18}F -FP-DTBZ concentration on the unlesioned side (unlesioned-ST/CB= 5.21 ± 0.38 , $n=3$) than the lesioned (lesioned-ST/CB= 2.34 ± 0.51). The results validated that ^{18}F -FP-DTBZ is a favorable PET ligand binding to VMAT2.

Key words VMAT2, Imaging agent, ^{18}F -FP-DTBZ, Synthesis, Biodistribution, MicroPET, Parkinson's disease

1 Introduction

In the central nervous system, vesicular monoamine transporter 2 (VMAT2) locates in the presynaptic monoaminergic terminals and plays a critical role for the movement of monoamine neurotransmitters (dopamine, norepinephrine, serotonin) from the cytosol into the storage vesicle lumen. Imaging VMAT2 with PET (positron emission tomography) in the brain provides a non-invasive measurement to reflect integrity of the three monoaminergic neurons. This reflection is helpful for diagnosing and monitoring of VMAT2 related disorders such as Parkinson's disease (PD) and Huntington's disease.

^{11}C labeled racemic dihydrotetrabenazine, including (\pm)- ^{11}C -DTBZ and its bioactive isomer, (+)- ^{11}C -DTBZ, are favorable PET ligand for human VMAT2 visualization. In the past decades, the two tracers were successfully used for mapping or tracing VMAT2 in the central nervous system and in the β -cell mass of the pancreas^[1-11]. However, with a half-life of $t_{1/2}=20$ min, ^{11}C labeled radiopharmaceutical must be prepared with an on-site medical cyclotron, which limited wide application of the tracers. The radionuclide ^{18}F ($t_{1/2}=110$ min) labeled DTBZ analogs with similar or better affinity and selectivity to VMAT2 may provide convenient alternatives for clinical applications. In 2006, Goswami R, *et al.*^[12] reported two fluoroalkyl derivatives of dihydrotetrabenazine, ^{18}F -9-fluoroethyl-9-desmethyl-

Supported by the National Natural Science Foundation of China (30970844), the Outstanding Medical Professionals Foundation of Jiangsu Province (RC2011096) and Natural Science Foundation of Jiangsu Province of China (BK2010155).

* Corresponding author. E-mail address: czp72@163.com

Received date: 2011-07-18

DTBZ (^{18}F -FE-DTBZ) and ^{18}F -9-fluoropropyl-9-desmethyl-DTBZ (^{18}F -FP-DTBZ).

Initial investigation revealed that the ^{18}F -FP-DTBZ had similar, or somehow better, specific binding to VMAT2 than (+)-DTBZ^[12,13]. The results suggested possibility of ^{18}F labeled DTBZ derivatives as potential PET ligands for VMAT2 tracing. In this paper, we report a semi-automated radiosynthesis of ^{18}F -FP-DTBZ and validated its potential by brain biodistribution and microPET studies in rats.

2 Materials and method

Mesylate precursor of ^{18}F -FP-DTBZ, (\pm)-2-Hydroxy-3-isobutyl-9-(3-methanesulfonyloxypropoxy)-10-methoxy-1,2,3,4,6,7-hexahydro-11bH-benzo[a]quinolizine (MsOP-DTBZ), was synthesized in our laboratory according to the methods in Ref.[12]. DTBZ, a VMAT2 inhibitor, was prepared using the method in Ref.[14]. The 2 β -carbomethoxy-3 β -(4-fluorophenyl) nortropane (CFT), a dopamine transporter inhibitor, was synthesized as previously reported^[15]. The analytical HPLC system for characterizing ^{18}F -FP-DTBZ included a binary HPLC pump (Waters 1525, USA), a UV detector (Waters 2487, USA) and a flow scintillation analyzer (Radiomatic 610TR, Perkin-Elmer, USA). All Sprague-Dawley rats were purchased from Shanghai SLAC Laboratory Animal Center. The 6-Hydroxydopamine (6-OHDA) was purchased from Sigma Co. and the left-sided 6-OHDA lesioned PD rats were established as previously described^[16].

2.1 Radiosynthesis of ^{18}F -FP-DTBZ

Semi-automated radiosynthesis of ^{18}F -FP-DTBZ was carried out on a ^{18}F -multifunction synthesizer (Beijing PET Technology Co. Ltd., China) with a computer interface as described previously^[17]. ^{18}F was produced with a HM-7 cyclotron (Sumitomo Heavy Industries, Ltd., Japan) and trapped in a QMA cartridge (Waters, USA). ^{18}F -FP-DTBZ was prepared using a method modified from those in Ref.[12].

[^{18}F]-fluorination began with elution of ^{18}F (9.25–12.95 GBq) in QMA cartridge by feeding 1.0 mL stock solution (containing 13 mg K222 in 0.8 mL CH_3CN and 2 mg K_2CO_3 in 0.2 mL water) to a reaction tube under N_2 pressure. The solution was

heated under N_2 at 105°C to evaporate solvent followed by azeotropic evaporation using acetonitrile (1.0 mL) in air bath at 105°C. The residue was cooled below 50°C, followed by addition of 2.0 mg precursor (MsOP-DTBZ, in 1.5 mL 3:2 DMF/acetonitrile). The obtained solution was mixed by N_2 flow and heated at 110°C for 8 min. The crude product was diluted with 3.5 mL semi-preparation HPLC elution and loaded onto an Alltima 10 \times 200 mm C_{18} column (Alltech, USA). The column was eluted with 1:2 ($\text{CH}_3\text{CN}/50$ mM NH_4Ac , pH 4.5) at a flow rate of 3 mL/min. The elution was monitored by a radio detector fixed on the synthesizer. Fraction containing ^{18}F -FP-DTBZ was collected and diluted with 60 mL water. The diluted solution was then transferred to a Sep-Pak C_{18} cartridge (pre-activated with 20 mL ethanol followed by 20 mL water) to trap ^{18}F -FP-DTBZ only. Then the C_{18} cartridge was rinsed with 10 mL water to remove organic solvent and NH_4Ac followed with 2 mL EtOH to obtain the pure ^{18}F -FP-DTBZ. Aseptic injection was obtained by filtering the EtOH elution through a 0.2 μm filter (Pall Company, USA) into a sterile vial and diluted to suitable radioactive concentration with saline before use.

Radiochemical purity (RCP) of ^{18}F -FP-DTBZ was determined with analytical HPLC system using a Symmetry C_{18} reversed-phase column (5 μm , 4.6mm \times 150mm, Waters) eluted with 1:3 ($\text{CH}_3\text{CN}/50$ mmol $\cdot\text{L}^{-1}$ NH_4Ac , pH 4.5) at a flow rate of 1.0 mL $\cdot\text{min}^{-1}$. The cold compound, ^{19}F -FP-DTBZ, was coinjected and monitored with a UV detector at 280 nm. The specific activity (SA) was estimated by comparing the UV absorption (280 nm) of the identical radioactive ^{18}F -FP-DTBZ with the standard curve of the cold ^{19}F -FP-DTBZ. To evaluate the in vitro stability of ^{18}F -FP-DTBZ, RCP was determined every 1 hour after the radiosynthesis.

2.2 Biodistribution and blocking studies in rat brain

Twenty-four rats (220–250g) were divided into three groups: control, VMAT2 blocking and dopamine transporter (DAT) blocking group. Each group contained eight animals. Control rats were injected with 0.3 mL (11.1 MBq, at the first injection time)

^{18}F -FP-DTBZ *via* tail vein under diethyl ether anesthesia. All animals were decapitated under anesthesia at 60 min after injection. The interested brain regions, including cerebellum (CB), frontal cortex (FC), parietal cortex (PC), temporal cortex (TC), occipital cortex (OC), hippocampus (HP) and striatum (ST), were dissected, weighed and countered. The percentages of injected dose per gram (ID%/g) were calculated by a comparison of the tissue counts with suitably diluted aliquots of the injected dose. Rats for blocking study were coinjected with DTBZ (2 mg·kg⁻¹ body weight, in 0.2 mL EtOH/H₂O) to block VMAT2, or CFT (2 mg·kg⁻¹ body weight, in 0.2 mL EtOH/H₂O) to block dopamine transporter (DAT) and decapitated after 60 min post injection. The brain regions of interest were dissected, weighed and countered as described above. Data were presented as mean±SD. Statistical significance between groups was performed using unpaired Student's test. $P < 0.05$ was considered significant.

2.3 Micro-PET imaging

Imaging was performed using a Siemens Inveon 5000 micro-PET system. The energy resolution at 511 keV was 14.6% in average and in-plane radial and tangential resolutions were below 1.8-mm (FWHM) at center of FOV (field of view)^[18,19]. Three male 6-OHDA unilaterally lesioned rats and 3 control rats were used in the micro-PET study. Each was positioned prone on the micro-PET bed with head centered in the FOV and received 5.55–8.14 MBq ^{18}F -FP-DTBZ intravenously with a bonus injection via tail vein. An emission scan commenced immediately after injection and continued for 2 hours.

The obtained list mode data were histogrammed into 6×30s, 6×120s, 5×300s, 20×600s and reconstructed using 3D ordered subset expectation maximization (OSEM3D) after applying normalization, scatter, attenuation and sensitivity corrections. Frames from 9–30 min were summed to manually draw regions of interest (ROI) of the striatum because these frames showed relatively less nonspecific uptake. Three consecutive circular ROIs encompassing striatum (~30 mm³) on the coronal image were drawn and applied to all frames to generate time-activity curves (TACs). For the 6-OHDA lesioned rats in

which the lesioned striatum were not clearly visible, ROIs were drawn on the symmetrical position of the unlesioned striatum guided by the rat brain atlas^[20]. The cerebellum ROI (30–40 mm³) were obtained on three consecutive planes according to the atlas^[20]. All ROIs radioactivity were normalized to ID%/cm³ for plotting TACs.

3 Results and discussion

3.1 Radiosynthesis of ^{18}F -FP-DTBZ

To further evaluate the clinic potential of ^{18}F labeled DTBZ analogs, we firstly developed a semi-automated synthesis of ^{18}F -FP-DTBZ with an ^{18}F -multifunction synthesizer. ^{18}F -FP-DTBZ obtained here showed radiochemical purity (RCP) of over 98% and the same retention time (~7.2 min) as the cold compound, ^{19}F -FP-DTBZ (Fig.1), determined with analytical HPLC. The specific activity (SA) was estimated at over 1.3×10^{14} Bq·mmol⁻¹ at the end of synthesis. The whole synthesis duration was 60–70 min including the purification by semi-preparative HPLC and the radiochemical yield of ^{18}F -FP-DTBZ was 21%–35% without decay correction. However, chromatogram of the semi-preparation HPLC implicated that the fluorination yield in the reacted mixture might be over 75% (Fig.2), so optimal synthesis condition to minimize the radioactivity loss may dramatically increase the radiochemical yield of ^{18}F -FP-DTBZ.

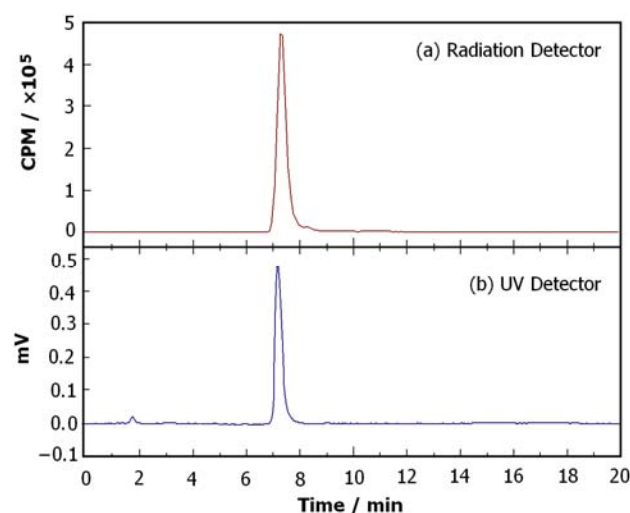


Fig.1 The chromatograms of purified ^{18}F -FP-DTBZ determined with a radiation detector and the co-injected ^{19}F -FP-DTBZ with a UV detector in the same analytical HPLC condition. ^{18}F -FP-DTBZ exhibited the same retention time as cold ^{19}F -FP-DTBZ.

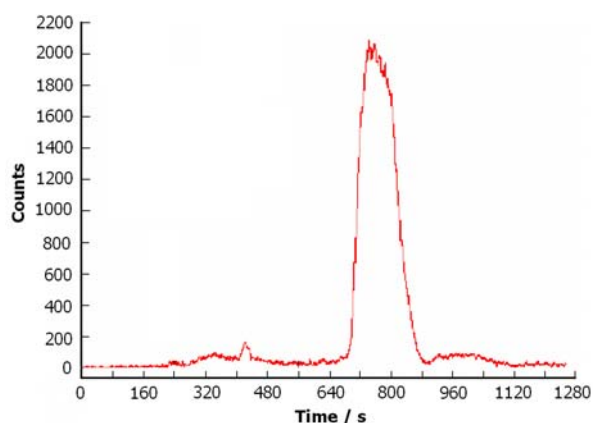


Fig.2 Semi-preparation HPLC chromatogram of the crude product monitored with a radioactivity detector. ^{18}F -FP-DTBZ, eluted between 700–880 s, showed a proportion of over 75% in the mixture.

Radiosynthesis reported here modified the method described by Goswami R, *et al.*^[12]. Firstly, during the purification of the crude ^{18}F -FP-DTBZ, Goswami R, *et al.* loaded the mixture onto an Oasis cartridge before semi-preparative HPLC purification. The cartridge was rinsed with water to remove the unreacted ^{18}F followed by acetonitrile to elute ^{18}F -FP-DTBZ. Our synthesis omitted the Oasis cartridge: the reacted mixture was directly loaded onto the column after filtration. The semi-preparative HPLC condition provided effective separation of the unreacted ^{18}F from ^{18}F -FP-DTBZ, which was confirmed by the chromatogram of analytical HPLC (Fig.1, unreacted ^{18}F was not visible at its retention time of 2.0–3.2 min). The omission is helpful for stable automated radiosynthesis and might facilitate clinic application. Second, in order to remove acetonitrile and NH_4Ac in the HPLC fraction, Sep-Pak C_{18} cartridge (Waters Co. USA) was applied to extract the ^{18}F -FP-DTBZ only, whereas acetonitrile, NH_4Ac and presumably minimal unreacted ^{18}F on the cartridge were washed out with 10 mL water. The pure ^{18}F -FP-DTBZ was obtained by rinsing the C_{18} cartridge with 2 mL EtOH. This solid-phase purification method has been successfully applied in some other ^{18}F labeled tracer injection preparation in clinical application instead of evaporating the solvent^[17,21,22]. The final ^{18}F -FP-DTBZ product, synthesized as described here, kept a RCP of >98% in 8 hours after the synthesis, which indicated its good in vitro stability.

3.2 Biodistribution and blocking studies in rats brain

To evaluate affinity of ^{18}F -FP-DTBZ to VMAT2 in the brain, biodistribution experiments were performed in rats. Significant localization of ^{18}F -FP-DTBZ in VMAT2 enriched regions, the striata (ST), was observed. As expected, the highest radioactive concentration was demonstrated in the ST ($0.67 \pm 0.12 \text{ ID}\% \cdot \text{g}^{-1}$ at 60 min post injection, mean \pm SD, $n=8$) and lowest in the cerebellum ($0.14 \pm 0.02 \text{ ID}\% \cdot \text{g}^{-1}$). The ST uptake is predominantly due to dopaminergic innervation. Low localization was also observed in the cortexes (FC: $0.17 \pm 0.02 \text{ ID}\% \cdot \text{g}^{-1}$; PC: $0.17 \pm 0.03 \text{ ID}\% \cdot \text{g}^{-1}$; OC: $0.15 \pm 0.02 \text{ ID}\% \cdot \text{g}^{-1}$; TC: $0.16 \pm 0.02 \text{ ID}\% \cdot \text{g}^{-1}$) and hippocampus ($0.17 \pm 0.02 \text{ ID}\% \cdot \text{g}^{-1}$). Ratio of target (ST) to nontarget (CB, commonly used as background) was 4.81 ± 0.84 at 60min post injection. These results are consistent with the experience of Michael R *et al.*, in which a bonus and constant infusion administration of ^{18}F -FP-DTBZ is adopted^[13], and also correlate with the brain distribution in mice reported by Goswami R^[12]. Accumulation of radioactivity in VMAT2-enriched ST tissue validated high affinity of ^{18}F -FP-DTBZ to VMAT2.

Specificity of ^{18}F -FP-DTBZ was validated by blocking experiments. When co-injected with 2 mg/kg DTBZ, a VMAT2 inhibitor, ^{18}F -FP-DTBZ displayed dramatically decreased localization in the striatum compared with the control rats (0.18 ± 0.03 vs. $0.67 \pm 0.12 \text{ ID}\% \cdot \text{g}^{-1}$, $P < 0.001$, $n=8$, Fig.3). Significant decrease was also observed in the HP ($P < 0.05$), which may be related to the VMAT2 sites of serotonin neuronal terminals in this region. No significant variance was observed in cortexes and cerebellum, regions lack of VMAT2 ($P > 0.1$, Fig.3). By contrast, rats co-injected with CFT, a DAT inhibitor, showed non-significant increase of ^{18}F -FP-DTBZ uptake in all interested brain regions compared with the control group ($P > 0.1$, Fig.3). We also found that the total brain uptake displayed significant decrease in DTBZ group (0.18 ± 0.03 vs. $0.31 \pm 0.04 \text{ ID}\%$, $P < 0.001$, $n=8$) and increase in CFT group (0.37 ± 0.17 vs. $0.31 \pm 0.04 \text{ ID}\%$, $P < 0.05$) compared with control group. The decreased brain uptake of DTBZ group, which consistent with the results in mice reported by Goswami R *et al.*^[12],

may due to the blocking of VMAT2 in the brain, and the increased brain uptake in CFT group, which is similar to the results of raclopride (a dopamine D2 receptor inhibitor) coinjected group in mice reported by Goswami R, *et al.*^[12], may due to the increased dopamine concentration in dopaminergic synapse cleft. Although further investigation in larger scale is needed to verify and clarify the mechanism of the varied brain uptakes, the ¹⁸F-FP-DTBZ binding specificity to VMAT2 was thus confirmed by blocking experiments.

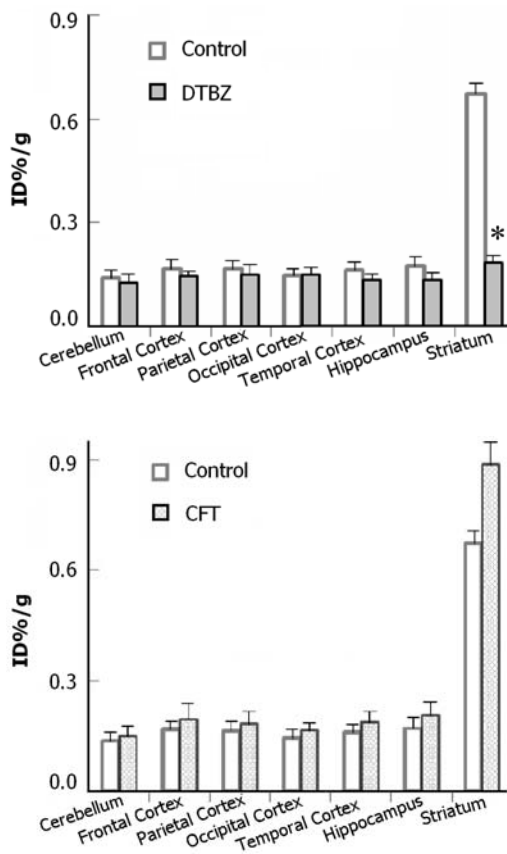


Fig.3 Brain biodistribution of ¹⁸F-FP-DTBZ at 60 min post injection in control rats and pretreated with DTBZ or CFT (**P*<0.001 versus control group). Data were presented as mean±*SD* for *n*=8 animals.

3.3 Micro-PET imaging

To confirm *in vivo* affinity and specificity of ¹⁸F-FP-DTBZ, microPET imaging was performed in normal and 6-OHDA unilaterally lesioned rats. The 6-OHDA stereoselectively lesioned rat, used in this study, is a traditional PD model not only for preclinical studies of dopamine transmission related diseases but also for feasibility assessment of potential ligand^[16,23,24].

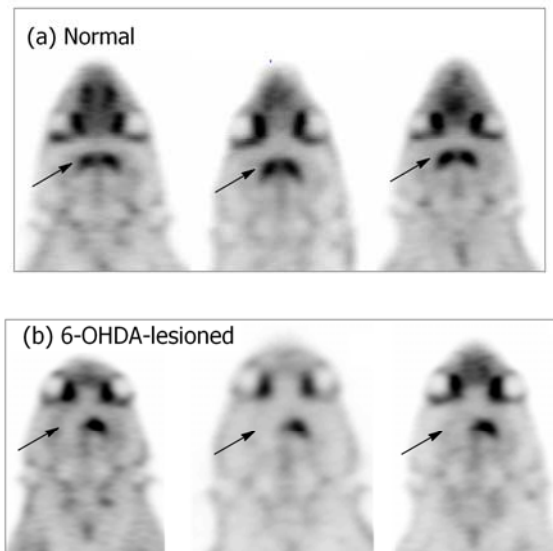


Fig.4 MicroPET brain images of normal and 6-OHDA left-lesioned PD rat, imaged with ¹⁸F-FP-DTBZ. The images were reconstructed with OSEM3D and summed from 9 to 30 min post injection for this illustration.

As shown in Fig.4, microPET in normal rats resulted in images where both striata could be recognized symmetrically with confidence, as there was high contrast with respect to other cerebral structures. By contrast, the 6-OHDA treated rats gave a total or partial decrease in radioactivity uptake in the lesioned side, whilst the unlesioned side displayed relative higher uptake. The decrease resulted in invisibility of the lesioned striatum image due to low contrast with other cerebral structures (Fig.4). Non-specific binding were seen in nasal cavity and hardierian glands in all frames, but not in the brain especially in later frames. These imaging results *in vivo* confirmed high affinity and specificity of ¹⁸F-FP-DTBZ to VMAT2.

To investigate dynamical VMAT2 binding of ¹⁸F-FP-DTBZ, TACs were generated by ROI analysis. As presented in Fig.5, the control rats gave high and almost symmetrical ¹⁸F-FP-DTBZ uptake in left and right striatum, whereas the 6-OHDA pretreated rats gave dramatically decreased uptake in the lesioned side. In addition, ¹⁸F-FP-DTBZ displayed good retention in ST and rapid clearance in CB, resulting in much higher radioactivity than cerebellum after 10 min post injection. Assessment of the TACs suggested a selection of the time window for quantitation, which in the case of rats could be from 80 to 120 min. During

this interval, the target-to-nontarget (ST/CB) ratio value reached maximum of 5.08 ± 0.81 (mean \pm SD, $n=3$) in control rats, whereas the unlesioned-ST/CB and lesioned-ST/CB ratio in 6-OHDA treated rats reached 5.21 ± 0.38 and 2.34 ± 0.51 ($n=3$), respectively. All these results from TACs *in vivo* validate high affinity, high specificity and favorable pharmacokinetics of ^{18}F -FP-DTBZ as a VMAT2 tracer for PET imaging. Further study to synthesize (+)- ^{18}F -FP-DTBZ, the bioactive component in racemic enantiomers as prepared here (containing theoretically 50% (+)- ^{18}F -FP-DTBZ and 50% (–)- ^{18}F -FP-DTBZ)^[25–28], and to investigate its selectivity were ongoing.

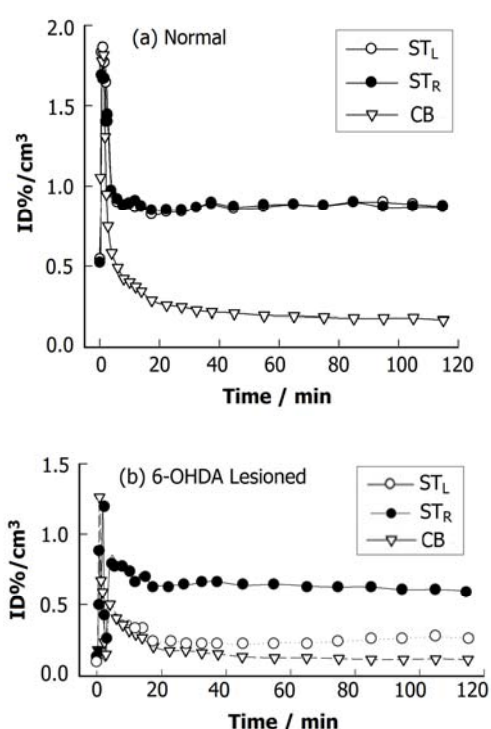


Fig.5 Time-activity curves of the left striatum (ST_L), right striatum (ST_R) and cerebellum (CB) ROIs in normal and 6-OHDA left lesioned PD rat injected with ^{18}F -FP-DTBZ intravenously.

4 Conclusion

In summary, radiosynthesis and purification of ^{18}F -FP-DTBZ reported here provided a reliable method for preparing high-purity ^{18}F -FP-DTBZ. Biodistribution, blocking and microPET studies validated that ^{18}F -FP-DTBZ has favorable affinity and selectivity to VMAT2. These results suggest that ^{18}F -FP-DTBZ is a potential ^{18}F labeled ligand to assess VMAT2 integrity.

Acknowledgements

The authors would like to acknowledge YU Shanyou, LU Chen and GUO Xianwei for their technical assistance.

References

- 1 DaSilva J N, Kilbourn M R, Mangner T J. *Appl Radiat Isot*, 1993, **44**: 673–676.
- 2 Kilbourn M, Lee L, Borghet T V, *et al.* *Eur J Pharmacol*, 1995, **278**: 249–252.
- 3 Frey K A, Koeppe R A, Kilbourn M R, *et al.* *Ann Neurol*, 1996, **40**: 873–884.
- 4 Koeppe R A, Frey K A, VanderBorghet T M, *et al.* *J Cereb Blood Flow Metab*, 1996, **16**: 1288–1299.
- 5 Bohnen N I, Minoshima S, Kilbourn M R, *et al.* *Neurology*, 1999, **52**: A176–A176.
- 6 Chan G L Y, Holden J E, Stoessl A J, *et al.* *J Nucl Med*, 1999, **40**: 283–289.
- 7 Martin W R, Wieler M, Stoessl A J, *et al.* *Ann Neurol*, 2008, **63**: 388–394.
- 8 Simpson N R, Souza F, Witkowski P, *et al.* *Nucl Med Biol*, 2006, **33**: 855–864.
- 9 Freeby M, Goland R, Ichise M, *et al.* *Diabetes Obes Metab*, 2008, **10**: 98–108.
- 10 Inabnet W B, Milone L, Harris P, *et al.* *Surgery*, 2010, **147**: 303–309.
- 11 Fagan S P, Fischman A J. *J Nucl Med*, 2009, **50**: 335–337.
- 12 Goswami R, Ponde D E, Kung M P, *et al.* *Nucl Med Biol*, 2006, **33**: 685–694.
- 13 Kilbourn M R, Hockley B, Lee L, *et al.* *Nucl Med Biol*, 2007, **34**: 233–237.
- 14 Whittaker N J. *Chem Soc C*, 1969: 85–89.
- 15 Li X M, Chen Z P, Fu R G, *et al.* *Chem Reagents*, 2004, **26**: 185–186 (in Chinese).
- 16 Wang S, Chen Z, Li X, *et al.* *Nucl Sci Techniques*, 2009, **20**: 11–16.
- 17 Chen Z P, Wang S P, Li X M, *et al.* *Appl Radiat Isot*, 2008, **26**: 1881–1885.
- 18 Visser E P, Disselhorst J A, Brom M, *et al.* *J Nucl Med*, 2009, **50**: 139–147.
- 19 Bao Q, Newport D, Chen M, *et al.* *J Nucl Med*, 2009, **50**: 401–408.
- 20 Paxinos G, Watson C. *The Rat Brain in Stereotaxic Coordinates*. London: Academic Press, 2007.
- 21 Voll R J, McConathy J, Waldrep M S, *et al.* *Appl Radiat Isot*, 2005, **63**: 353–361.

- 22 Zhu L, Liu Y, Plossl K, *et al.* Nucl Med Biol, 2010, **37**: 133–41.
- 23 Li X M, Chen Z P, Wang S P, *et al.* Nucl Sci Techniques, 2007, **18**: 223–226.
- 24 Collantes M, Penuelas I, Alvarez-Erviti L, *et al.* Rev Esp Med Nucl, 2008, **27**: 103–111.
- 25 Lin K J, Weng Y H, Wey S P, *et al.* J Nucl Med, 2010, **51**: 1480–1485.
- 26 Hefti F F, Kung H F, Kilbourn M R, *et al.* PET Clinics, 2010, **5**: 75–82.
- 27 Kung M P, Hou C, Goswami R, *et al.* Nucl Med Biol, 2007, **34**: 239–246.
- 28 Tsao H H, Lin K J, Juang J H, *et al.* Nucl Med Biol, 2010, **37**: 413–419.